

Whole-Body Distribution and Radiation Dosimetry of ^{11}C -Elacridar and ^{11}C -Tariquidar in Humans

Martin Bauer¹, Matthias Blaickner^{1,2}, Cécile Philippe³, Wolfgang Wadsak³, Marcus Hacker³, Markus Zeitlinger¹, and Oliver Langer¹⁻³

¹Department of Clinical Pharmacology, Medical University of Vienna, Vienna, Austria; ²Health and Environment Department, AIT Austrian Institute of Technology GmbH, Seibersdorf, Austria; and ³Division of Nuclear Medicine, Department of Biomedical Imaging and Image-Guided Therapy, Medical University of Vienna, Vienna, Austria

^{11}C -elacridar and ^{11}C -tariquidar are new PET tracers to assess the transport activity of P-glycoprotein (adenosine triphosphate-binding cassette subfamily B, member 1 [ABCB1]) and breast cancer resistance protein (adenosine triphosphate-binding cassette subfamily G, member 2 [ABCG2]). This study investigated the whole-body distribution and radiation dosimetry of both radiotracers in humans. **Methods:** Twelve healthy volunteers (6 women, 6 men) underwent whole-body PET/CT imaging over the 90 min after injection of either ^{11}C -elacridar or ^{11}C -tariquidar. Radiation doses were calculated with OLINDA/EXM software using adult reference phantoms. **Results:** Biodistribution was consistent with a major elimination route of hepatobiliary excretion, which may be mediated by ABCB1 and ABCG2. High radioactivity uptake was seen in liver, followed by spleen and kidneys, whereas brain uptake was lowest. Effective doses were $3.41 \pm 0.06 \mu\text{Sv}/\text{MBq}$ for ^{11}C -elacridar and $3.62 \pm 0.11 \mu\text{Sv}/\text{MBq}$ for ^{11}C -tariquidar. **Conclusion:** Our data indicate that both ^{11}C -elacridar and ^{11}C -tariquidar are safe radiotracers, for which an injected activity of 400 MBq corresponds to a total effective dose of approximately 1.5 mSv.

Key Words: P-glycoprotein; breast cancer resistance protein; radiation dosimetry; ^{11}C -elacridar; ^{11}C -tariquidar

J Nucl Med 2016; 57:1265–1268

DOI: 10.2967/jnumed.116.175182

The transporters P-glycoprotein (adenosine triphosphate-binding cassette subfamily B, member 1 [ABCB1]) and breast cancer resistance protein (adenosine triphosphate-binding cassette subfamily G, member 2 [ABCG2]) are highly expressed in excretory organs (liver, kidney, intestine) and at blood–tissue barriers (blood–brain [BBB], blood–testis, blood–placenta, and blood–retina) (1). These transporters are capable of transporting drugs and drug metabolites. They can therefore influence drug disposition, such as by mediating hepatobiliary and renal excretion and by controlling intestinal absorption of drugs. At the BBB, ABCB1 and ABCG2 work together in limiting brain distribution of dual

ABCB1/ABCG2 substrate drugs, such as tyrosine kinase inhibitors (2). ABCB1/ABCG2-mediated efflux transport is an important reason why many drugs fail to achieve therapeutically effective concentrations in the brain. Alteration of ABCB1 and ABCG2 transport activity in different organs by polymorphisms in the genes encoding ABCB1 and ABCG2, by drug–drug interactions, and by disease-induced mechanisms can lead to variability in the pharmacokinetics of ABCB1/ABCG2 substrate drugs and may have important consequences for drug safety and efficacy (1).

PET with radiolabeled ABCB1 substrates, such as ^{11}C -verapamil and ^{11}C -N-desmethyl-loperamide, has proven useful for assessing ABCB1 function at the BBB (3). To our knowledge, no PET tracers are available yet to measure ABCG2 function at the BBB. We introduced ^{11}C -elacridar and ^{11}C -tariquidar as a new class of radiotracer to measure both ABCB1 and ABCG2 function at the BBB (4–7). ABCB1 and ABCG2 may influence the pharmacokinetics of ^{11}C -elacridar and ^{11}C -tariquidar not only in the brain but also in peripheral organs such as the liver, thus potentially enabling assessment of transport activity in these organs. This study used PET/CT to investigate the whole-body distribution and radiation dosimetry of ^{11}C -elacridar and ^{11}C -tariquidar in healthy volunteers.

MATERIALS AND METHODS

Subjects

The study was registered with EudraCT, the European Clinical Trials Database (number 2010-020759-30), and approved by the Ethics Committee of the Medical University of Vienna. Twelve healthy volunteers with no evidence of renal or hepatic dysfunction and no history of surgery were included. Six women (mean age \pm SD, 28.6 ± 7.2 y; mean weight, 60.7 ± 4.9 kg) and 6 men (mean age, 25.6 ± 1.6 y; mean weight, 73.3 ± 5.6 kg) were randomly assigned to receive either ^{11}C -elacridar ($n = 3$ per sex) or ^{11}C -tariquidar ($n = 3$ per sex).

Radiotracer Synthesis

^{11}C -elacridar and ^{11}C -tariquidar were synthesized as previously described (6). The specific activities at the time of injection were 62.6 ± 45.1 GBq/mmol for ^{11}C -elacridar and 19.6 ± 1.9 GBq/mmol for ^{11}C -tariquidar, with radiochemical purity exceeding 97%.

PET/CT Protocol

All scanning was performed on a Biograph TruePoint 64 PET/CT scanner (Siemens Healthcare USA). The subjects were positioned on a vacuum mattress to minimize movement artifacts. After a low-dose whole-body CT scan, ^{11}C -elacridar (400 ± 9 MBq) or ^{11}C -tariquidar

Received Mar. 2, 2016; revision accepted Mar. 11, 2016.

For correspondence or reprints contact: Martin Bauer, Department of Clinical Pharmacology, Medical University of Vienna, Währinger-Gürtel 18-20, 1090 Vienna, Austria.

E-mail: martin.m.bauer@meduniwien.ac.at

Published online Apr. 14, 2016.

COPYRIGHT © 2016 by the Society of Nuclear Medicine and Molecular Imaging, Inc.

(375 ± 57 MBq) was injected intravenously and a 30-min dynamic PET scan of brain, thorax, or lower abdomen was acquired ($n = 2$ per radiotracer and organ group, 1 man and 1 woman each). Thereafter, 2 whole-body scans, with a 3-min acquisition time per bed position for the first scan and 5 min for the second scan, were obtained. Depending on the subject's size, 5–6 bed positions were needed to scan from the middle of the thigh to the top of the head. At the end of the imaging study, the subjects were asked to empty their urinary bladders, and the radioactivity excreted into urine was measured using a γ -counter.

Image Analysis

PET/CT images were analyzed using the open-source software AMIDE. Volumes of interest were drawn on the fused PET/CT data around organs and tissues that had visible radioactivity uptake, including liver, gallbladder, kidneys, spleen, myocardium, urinary bladder, muscle (quadriceps femoris), small intestine, red bone marrow (L3 to L5), and brain. Dynamic PET data (the first 30 min of the scan) were available for only 2 subjects (1 man, 1 woman) per organ group (brain, thorax, or lower abdomen) and were assumed representative of the whole group. Furthermore, volumes of interest were applied to the static acquisitions recorded at 32.5 ± 1.2 min and 54.5 ± 2.5 min after radiotracer injection. For each volume of interest and each time point, the individual SUV was calculated. Time-activity curves were generated for each volume of interest, and the residence time, that is, the time-integrated activity coefficient according to the MIRD nomenclature, was calculated (8). For each subject, the organ masses were determined by scaling the organ masses of the respective reference phantoms (9) according to the subject's weight. The resulting residence times of the 5 source organs with the highest radioactivity concentrations, together with the remainder of the body, defined as the total number of disintegrations in the body minus the disintegrations in the aforementioned source organs, were used as input for the dose calculation with OLINDA/EXM (10). The results are presented as organ-equivalent doses and effective dose according to the definitions in publication 103 of the International Commission on Radiological Protection (11).

RESULTS

The acquisition protocol allowed for measurement of radio-tracer kinetics in a range of different organs. There was no indication that any subject moved between the low-dose CT and PET scans or during the PET scan. Typical coronal whole-body images of ^{11}C -elacridar and ^{11}C -tariquidar are shown in Figure 1. The time-activity curves for ^{11}C -elacridar and ^{11}C -tariquidar in individual organs averaged over all subjects are shown in Figures 2 and 3. All investigated organs except spleen displayed slow wash-out of radioactivity during the PET scan. Radioactivity concentrations measured in different organs in the whole-body scans did not significantly differ between men and women (2-way ANOVA). In 1 subject who received ^{11}C -elacridar and 5 subjects who received ^{11}C -tariquidar, the percentage of radioactivity excreted into urine was measured. For ^{11}C -elacridar, 0.8% of the injected dose was excreted, and for ^{11}C -tariquidar, $1.9\% \pm 0.6\%$ of the injected dose ($n = 4$) was excreted. The percentage of ^{11}C -tariquidar excreted into urine was markedly higher in one of the 5 subjects (18.8% injected dose); that subject had a markedly lower gallbladder SUV in the second whole-body scan than did the other 4 subjects (12.4 vs. 41.5 ± 30.7). Organ-equivalent and total effective doses for both radiotracers are given in Table 1. The organ with the highest radiation burden was liver, followed by spleen and kidneys.

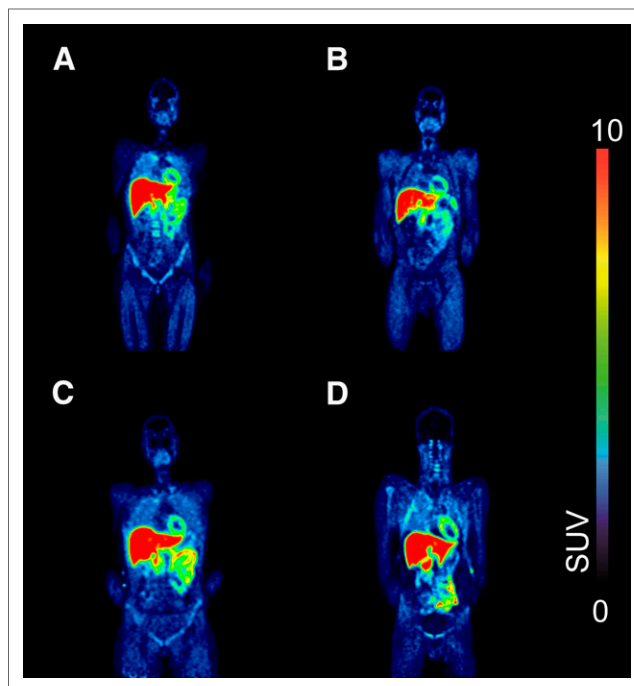


FIGURE 1. Coronal views showing biodistribution in representative subjects at 32.5 ± 1.2 min after injection: ^{11}C -elacridar in a woman (A) and a man (B) and ^{11}C -tariquidar in a woman (C) and a man (D). Scale is SUV from 0 to 10.

DISCUSSION

We studied the whole-body distribution of ^{11}C -elacridar and ^{11}C -tariquidar in healthy men and women. Elacridar and tariquidar were

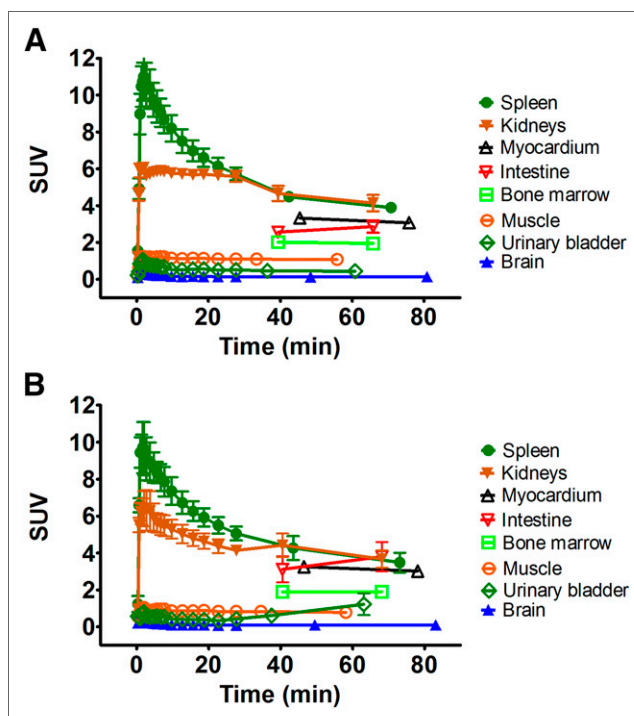


FIGURE 2. Time-activity curves ($\text{SUV}_{\text{mean}} \pm \text{SE of mean}$) for ^{11}C -elacridar (A) and ^{11}C -tariquidar (B) in different organs.

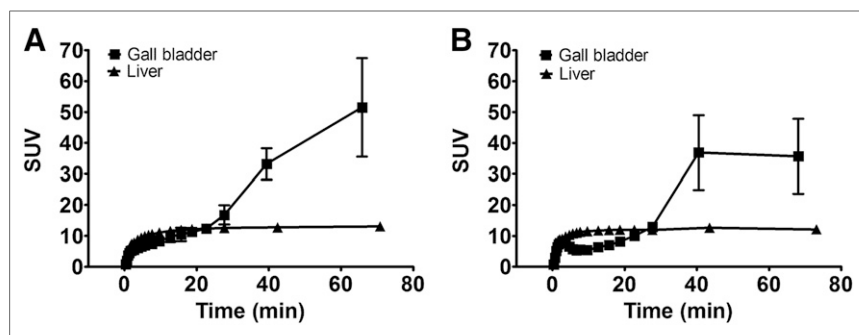


FIGURE 3. Time-activity curves ($SUV_{mean} \pm SE$ of mean) for ^{11}C -elacridar (A) and ^{11}C -tariquidar (B) in liver and gallbladder.

originally developed as third-generation ABCB1 inhibitors for use in cancer patients to overcome ABCB1-mediated multidrug resistance of tumors. Later, elacridar and tariquidar were also found to inhibit ABCG2 (12,13). We and others found that elacridar and tariquidar—in microdoses as used for PET—are substrates of murine and human ABCB1 and ABCG2 and undergo only negligible metabolism (4–7,14,15). ^{11}C -elacridar and ^{11}C -tariquidar can be used to assess ABCB1 and ABCG2 function at the rodent and human BBB (4–7). Because ABCB1 and ABCG2 are also expressed in clearance organs (liver, kidney, intestine), they can influence the pharmacokinetics of drugs. A PET method to assess ABCB1 and ABCG2 function in different organs would therefore be of great interest in drug development.

The whole-body distribution of ^{11}C -elacridar and ^{11}C -tariquidar was characterized by a high radioactivity concentration in liver, gallbladder, and intestine and a negligible radioactivity concentration in urinary bladder, suggesting that biliary excretion and possibly intestinal secretion are major routes of elimination of these radiotracers (Fig. 1). The rise in gallbladder radioactivity over the course of the PET experiment (Fig. 3) supports the possibility that both of the radiotracers or their radiolabeled metabolites are

excreted into bile. A previous study assessed the effect of increasing doses of unlabeled tariquidar on whole-body distribution of ^{11}C -tariquidar in mice and found a dose-dependent decrease in the radioactivity recovered from the small intestine (14). This result suggests a saturable, transporter-mediated mechanism of biliary excretion or intestinal secretion. ABCB1 and ABCG2 may be involved in these processes because these transporters are expressed both in the canalicular membrane of hepatocytes and in the luminal membrane of intestinal epithelial cells, where they transport drugs and drug metabolites from hepatocytes into bile

canalculi or from blood directly into the intestine (1). Consistent with previous studies, the lowest distribution of radioactivity was to the brain, as can be explained by ABCB1- and ABCG2-mediated efflux transport at the BBB (6,7). The time-activity curves for ^{11}C -elacridar and ^{11}C -tariquidar in all studied organs except spleen were characterized by a slow washout, which may be due to intracellular acidic trapping of the weak bases elacridar and tariquidar in lysosomes (16).

The highest dose was received by liver, followed by spleen and kidneys, and these doses were considerably higher than those to blood-forming organs, gonads, or whole body (Table 1). Observed sex differences can most likely be attributed to the differing S values, reflecting differing anatomy, in the female and male reference phantoms used in OLINDA/EXM. The measured average effective doses for ^{11}C -elacridar and ^{11}C -tariquidar were within the same range as observed for other ^{11}C -tracers (17).

CONCLUSION

We determined an average whole-body exposure of $3.41 \pm 0.06 \mu Sv/MBq$ for ^{11}C -elacridar and $3.62 \pm 0.11 \mu Sv/MBq$ for

TABLE 1
Organ-Equivalent and Effective Doses for ^{11}C -Elacridar and ^{11}C -Tariquidar

Organ	^{11}C -elacridar		^{11}C -tariquidar	
	Women	Men	Women	Men
Gallbladder	5.74 ± 0.20	4.47 ± 0.14	5.79 ± 0.25	5.53 ± 0.37
Liver	33.10 ± 1.46	22.20 ± 0.98	30.10 ± 1.91	33.60 ± 2.77
Kidneys	13.20 ± 0.58	12.00 ± 0.58	14.70 ± 0.88	12.80 ± 0.33
Intestine	2.58 ± 0.11	2.13 ± 0.05	2.95 ± 0.11	1.86 ± 0.04
Spleen	16.70 ± 0.94	11.20 ± 0.43	15.50 ± 1.06	10.70 ± 0.43
Myocardium	3.07 ± 0.12	2.28 ± 0.05	3.47 ± 0.13	2.22 ± 0.10
Muscle	3.65 ± 0.19	2.89 ± 0.04	2.73 ± 0.17	2.79 ± 0.12
Brain	1.38 ± 0.08	1.07 ± 0.03	2.00 ± 0.09	0.65 ± 0.01
Red marrow	4.19 ± 0.16	2.93 ± 0.12	4.11 ± 0.14	3.04 ± 0.17
Gonads	2.40 ± 0.12	1.41 ± 0.04	2.78 ± 0.11	1.01 ± 0.02
Remainder of body*	3.45 ± 0.13	2.82 ± 0.05	2.93 ± 0.13	2.69 ± 0.17
Effective dose*	3.89 ± 0.07	2.92 ± 0.04	4.06 ± 0.08	3.19 ± 0.13

*According to publication 103 of the International Commission on Radiological Protection (11).
Data are mean $\mu Sv/MBq \pm SD$.

^{11}C -tariquidar, corresponding to a total effective dose of approximately 1.5 mSv for an injected activity of 400 MBq.

DISCLOSURE

The costs of publication of this article were defrayed in part by the payment of page charges. Therefore, and solely to indicate this fact, this article is hereby marked “advertisement” in accordance with 18 USC section 1734. This study was supported by grants KLI 139-B00, KLI 480-B30, and F 3513-B20 from the Austrian Science Fund (FWF) and grant 201380 from the European Community’s Seventh Framework program. No other potential conflict of interest relevant to this article was reported.

ACKNOWLEDGMENTS

We thank the staff of the PET/CT unit in the Division of Nuclear Medicine (Georg Dobrozemsky, Bettina Reiterits, Benedikt Schmiedinger, Barbara Straubinger, Katja Salzmann, Gabriele Wagner, and Georgios Karanikas) and the study nurse, Maria Weber, for their support.

REFERENCES

- Giacomini KM, Huang SM, Tweedie DJ, et al. Membrane transporters in drug development. *Nat Rev Drug Discov*. 2010;9:215–236.
- Agarwal S, Hartz AM, Elmquist WF, Bauer B. Breast cancer resistance protein and P-glycoprotein in brain cancer: two gatekeepers team up. *Curr Pharm Des*. 2011;17:2793–2802.
- Wanek T, Mairinger S, Langer O. Radioligands targeting P-glycoprotein and other drug efflux proteins at the blood–brain barrier. *J Labelled Comp Radiopharm*. 2013;56:68–77.
- Wanek T, Kuntner C, Bankstahl JP, et al. A novel PET protocol for visualization of breast cancer resistance protein function at the blood–brain barrier. *J Cereb Blood Flow Metab*. 2012;32:2002–2011.
- Bankstahl JP, Bankstahl M, Römermann K, et al. Tariquidar and elacridar are dose-dependently transported by p-glycoprotein and bcrp at the blood–brain barrier: a small-animal positron emission tomography and in vitro study. *Drug Metab Dispos*. 2013;41:754–762.
- Bauer M, Karch R, Zeitlinger M, et al. Interaction of ^{11}C -tariquidar and ^{11}C -elacridar with P-glycoprotein and breast cancer resistance protein at the human blood–brain barrier. *J Nucl Med*. 2013;54:1181–1187.
- Bauer M, Römermann K, Karch R, et al. A pilot PET study to assess the functional interplay between ABCB1 and ABCG2 at the human blood–brain barrier. *Clin Pharmacol Ther*. March 3, 2016 [Epub ahead of print].
- Bolch WE, Eckerman KF, Sgouros G, Thomas SR. MIRD pamphlet no. 21: a generalized schema for radiopharmaceutical dosimetry—standardization of nomenclature. *J Nucl Med*. 2009;50:477–484.
- Coffey JL, Cristy M, Warner GG. Specific absorbed fractions for photon sources uniformly distributed in the heart chambers and heart wall of a heterogeneous phantom. *J Nucl Med*. 1981;22:65–71.
- Stabin MG, Sparks RB, Crowe E. OLINDA/EXM: the second-generation personal computer software for internal dose assessment in nuclear medicine. *J Nucl Med*. 2005;46:1023–1027.
- The 2007 Recommendations of the International Commission on Radiological Protection: ICRP publication 103. *Ann ICRP*. 2007;37:1–332.
- de Bruin M, Miyake K, Litman T, Robey R, Bates SE. Reversal of resistance by GF120918 in cell lines expressing the ABC half-transporter, MXR. *Cancer Lett*. 1999;146:117–126.
- Kannan P, Telu S, Shukla S, et al. The “specific” P-glycoprotein inhibitor tariquidar is also a substrate and an inhibitor for breast cancer resistance protein (BCRP/ABCG2). *ACS Chem Neurosci*. 2011;2:82–89.
- Kawamura K, Konno F, Yui J, et al. Synthesis and evaluation of [^{11}C]XR9576 to assess the function of drug efflux transporters using PET. *Ann Nucl Med*. 2010;24:403–412.
- Kawamura K, Yamasaki T, Konno F, et al. Evaluation of limiting brain penetration related to P-glycoprotein and breast cancer resistance protein using [^{11}C]GF120918 by PET in mice. *Mol Imaging Biol*. 2011;13:152–160.
- Kannan P, Brimacombe KR, Kreisl WC, et al. Lysosomal trapping of a radiolabeled substrate of P-glycoprotein as a mechanism for signal amplification in PET. *Proc Natl Acad Sci USA*. 2011;108:2593–2598.
- van der Aart J, Hallett WA, Rabiner EA, Passchier J, Comley RA. Radiation dose estimates for carbon-11-labelled PET tracers. *Nucl Med Biol*. 2012;39:305–314.